# Controlled Single-Cell Compression With a High-Throughput MEMS Actuator

Jennifer L. Walker<sup>®</sup>, *Graduate Student Member, IEEE*, Luke H. C. Patterson<sup>®</sup>, *Graduate Student Member, IEEE*, Evelyn Rodriguez-Mesa<sup>®</sup>, Kevin Shields, John S. Foster, Megan T. Valentine<sup>®</sup>,

Adele M. Doyle<sup>©</sup>, and Kimberly L. Foster, *Member, IEEE* 

Abstract—The electromagnetically actuated MEMS μHammer was used to evaluate the effects of mechanical impact on the membrane permeability, apoptotic induction, and proliferation of human neural progenitor cells. The µHammer enabled application of two strain magnitudes ( $\varepsilon = 42\%$  and 69%) for two strain durations (10  $\mu$ s and 100  $\mu$ s) to individual cells at unprecedented high strain rates ( $\dot{\varepsilon} \sim 200 \times 10^3 \text{ s}^{-1}$ ) and high throughput (up to 36,000 cells/min). This enables large numbers of cells to be analyzed and the effects of strain magnitude and duration to be decoupled. The magnitude of applied strain significantly affected cell membrane permeability shortly after compression, whereas the duration of strain significantly increased early apoptosis in cells 24 hours after compression. Strain magnitude also significantly affected cell quantity over a 70-hour period, despite no significant difference in the cell doubling times. Understanding the relationship between mechanical strain and cellular response will ultimately lead to improved diagnostics and treatment of high strain rate mechanical injury conditions such as Traumatic Brain Injury. [2020-0171]

Index Terms—Cellular impact, cell compression, microfluidic MEMS actuator, strain, traumatic brain injury.

# I. Introduction

RAUMATIC Brain Injury (TBI) afflicts nearly 2.6 million people in the United States each year, predominantly children, young adults, and the elderly and is one of the leading

Manuscript received May 15, 2020; accepted June 13, 2020. This work was supported by the National Science Foundation under Grant CBET-1631656 and Grant CMMI-1254893. Subject Editor R. Ghodssi. (Corresponding author: Jennifer L. Walker.)

Jennifer L. Walker and Luke H. C. Patterson are with the Department of Mechanical Engineering, University of California at Santa Barbara, Santa Barbara, CA 93106 USA (e-mail: jenniferwalker@ucsb.edu; lpatterson@ucsb.edu).

Evelyn Rodriguez-Mesa, Kevin Shields, and John S. Foster are with Owl Biomedical, Santa Barbara, CA 93117 USA (e-mail: evelyn@ owlbiomedical.com; kevin@owlbiomedical.com; john@owlbiomedical.com).

Megan T. Valentine is with the Department of Mechanical Engineering, Neuroscience Research Institute, University of California at Santa Barbara, Santa Barbara, CA 93106 USA, and also with the Center for Bioengineering, University of California at Santa Barbara, Santa Barbara, CA 93106 USA (e-mail: mtvale@ucsb.edu).

Adele M. Doyle is with the Neuroscience Research Institute, University of California at Santa Barbara, Santa Barbara, CA 93106 USA, and also with the Center for Bioengineering, University of California at Santa Barbara, Santa Barbara, CA 93106 USA (e-mail: adoyle@ucsb.edu).

Kimberly L. Foster was with the Department of Mechanical Engineering, University of California at Santa Barbara, Santa Barbara, CA 93106 USA. She is now with the School of Science and Engineering, Tulane University, New Orleans, LA 70118 USA (e-mail: klfoster@tulane.edu).

Color versions of one or more of the figures in this article are available online at http://ieeexplore.ieee.org.

Digital Object Identifier 10.1109/JMEMS.2020.3005514

causes of disability worldwide [1], [2]. TBI is segmented into two injury categories: primary and secondary. Primary injury consists of the immediate damage acquired during the trauma, e.g. focal contusion and hemorrhage. Secondary injury is linked to the resulting biomolecular cascade occurring over minutes to weeks after the trauma and leading to neurodegeneration. Long term effects of TBI include memory loss, changes in behavior, and increased risk of developing Alzheimer's disease [3].

Previous *in vivo* mechanical injury studies have provided insight into the pathophysiology of the secondary injury, identifying injury responses such as increased inflammation and cell death [4], as well as indicators of neuroprotection and even neurogenesis [5], [6]. However, these animal studies involved injury to a heterogenous cell population, comprised of neural and cardiovascular tissue, and systemic physiologic influences [7]. Therefore, the biomolecular effects of mechanical loading could not be traced to individual cell responses in these *in vivo* experiments. This lack of understanding of specific cell response to mechanical injury limits the design of effective cell-targeted therapies for diseases like TBI.

Cell response to impact injury is not well understood, in part due to limitations of existing *in vitro* methods and a lack of *in vivo* measurement options. Tools used to measure cell modulus (e.g. AFM and aspiration pipettes) apply low, constant strains (typically  $\varepsilon < 10\%$ ) and are low throughput (<100 cells/experiment) [8]. Use of microfluidic instruments has increased the throughput for cell rheology studies, but these devices are optimized for low strain magnitude and have poor repeatability for strain injury [9]. Stretchable substrates allow for variable strain magnitudes as high as  $\varepsilon = 130\%$  but can apply limited strain rates ( $\dot{\varepsilon} < 100 \text{ s}^{-1}$ ). Moreover, the strain is applied to a cell monolayer, not to individual cells [10]–[12].

To address this need for improved tools, we developed the  $\mu$ Hammer, an electromagnetically actuated MEMS device that is capable of applying mechanical strain to individual cells in vitro at unprecedented high strain rates ( $\dot{\epsilon} \sim 200 \times 10^3 \ s^{-1}$ ) [13], [14]. The  $\mu$ Hammer combines microfluidics with timegated electro-magnetic actuation to achieve high-throughput injury of up to 36,000 cells/minute, allowing both single cell and population averages to be calculated. After compression, cells can be recovered and returned to culture, allowing their functions and properties to be monitored over time.

1057-7157 © 2020 IEEE. Personal use is permitted, but republication/redistribution requires IEEE permission. See https://www.ieee.org/publications/rights/index.html for more information.

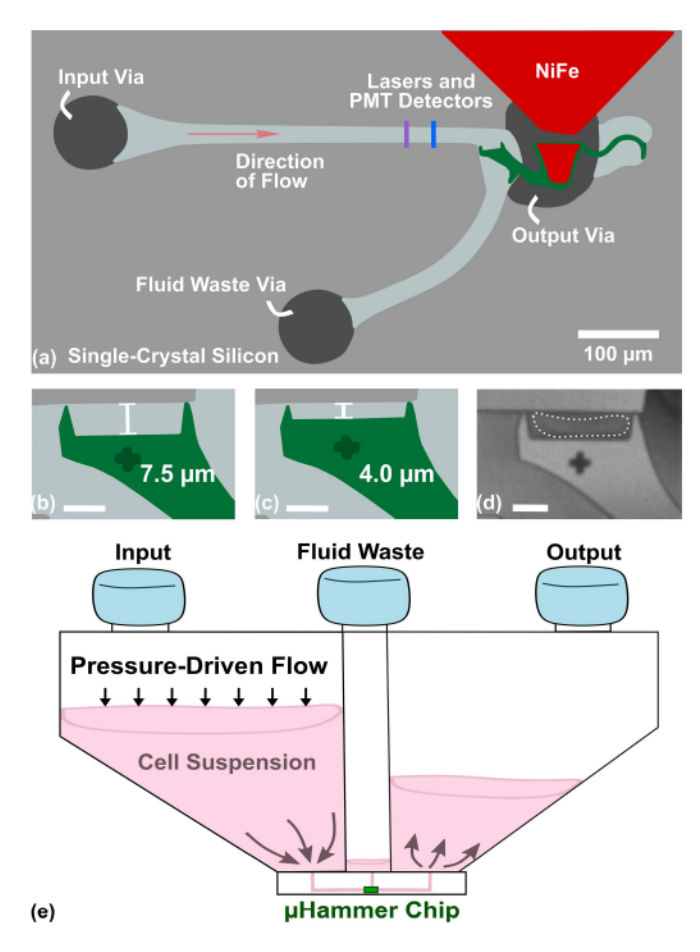


Fig. 1. (a) Schematic of the  $\mu$ Hammer chip, with magnetic system (red) and impact system (green). Schematics of the impact face for two fabricated  $\mu$ Hammers, closed to gap sizes of (b) 7.5  $\mu$ m and (c) 4.0  $\mu$ m, with 10  $\mu$ m scale bars. These gap sizes provide strains to NPCs of  $\varepsilon=42\%$  and  $\varepsilon=69\%$ , respectively. (d) Micrograph of a cell compressed by a 7.5  $\mu$ m gap  $\mu$ Hammer; cell is outlined by dashed white line. Scale bar is 10  $\mu$ m. (e) Illustration of  $\mu$ Hammer cartridge that interfaces with Owl biomedical's MACSQuant® Tyto® cell sorter and is bonded to the  $\mu$ Hammer chip.

Here we use the  $\mu$ Hammer to investigate the effects of compression on human Neural Progenitor Cells (NPCs, Millipore ReNcell VM cell line). By independently varying the applied strain magnitude and strain duration, the effects of these parameters on membrane permeability, early apoptosis, and proliferation can be assessed, and decoupled, providing insight into cell response to mechanical injury.

# II. METHODS

# A. The µHammer Device

As previously described by our group [13], [14], the  $\mu$ Hammer is a microchip device fabricated by Owl biomedical (USA), consisting of a microfluidic channel (25- $\mu$ m wide by 50- $\mu$ m deep), Ni-Fe magnetic system, and impact system (Fig. 1a). The magnetic system, shown in red, comprises the tapered Ni-Fe pole that interfaces with an external solenoid and the Ni-Fe armature, while the impact system, shown in green, includes the impact face and the S-curved spring.

For this work, we fabricated [14] two  $\mu$ Hammer devices, differing in the impact faces that set the minimum gap size when actuated to either 7.5  $\mu$ m (Fig. 1b) or 4.0  $\mu$ m (Fig. 1c),

In each device, the presence of pincers (Fig. 1c-e) dictates both the final gap size under full actuation and bursts off-center cells. A single cell captured in the 7.5  $\mu$ m gap  $\mu$ Hammer is shown in Fig. 1b.

The  $\mu$ Hammer chip is bonded to a sterilized cartridge (Fig. 1c) that interfaces with the MACSQuant® Tyto® (Miltenyi Biotech, Germany) which houses the external solenoid, two lasers (405 nm and 488 nm), and two photodetectors.

# B. The µHammer Device Working Principles

Cells suspended in fluid are pressure driven (60 kPa) through the microchip inlet via and the microfluidic channel at an average velocity of  $2.5 \pm 0.25$  m/s. Two lasers spaced 50- $\mu$ m apart are upstream of the impact face and as each cell crosses through each laser beam, the resulting backscatter is detected. From this, the cell velocity is determined and the timing of actuation is adjusted to capture each cell on the impact face as the  $\mu$ Hammer face closes against the channel wall.

The  $\mu$ Hammer is electromagnetically actuated: 5A of current is supplied to the external solenoid creating a magnetic field that saturates the tapered Ni-Fe pole at 1.6 T. The Ni-Fe armature of the impact system is attracted to the pole, closing the impact face at an average velocity of  $\nu \simeq 2.6$  m/s. The pincers flanking the  $\mu$ Hammer impact face maintain contact with the channel wall, trapping each detected cell between the impact face, pincers, and the wall until the actuation current is released. Cell strain duration is thereby controlled by the time interval of applied current, which is user-set to sustain desired static cell compression up to 1,000  $\mu$ s. Once the current is released, the S-curved spring (stiffness,  $\kappa \simeq 224$  N/m) retracts the  $\mu$ Hammer to its resting position and the cell passes to the output chamber for collection and analysis.

# C. Device Implementation With Neural Progenitor Cells

Human NPCs (ReNcell VM, Millipore, USA), an immortalized adherent cell line, were cultured according to the manufacturer's recommendations and passaged every 3 days. The mean diameter of an NPC is  $12.98 \pm 2.27~\mu$ m, measured via Beckman Coulter Multisizer 4e Coulter Counter, N=1,848 cells, similar across n=3 replicates. Prior to injection into the  $\mu$ Hammer cartridge, the cells were resuspended in Tyto Running Buffer<sup>TM</sup> (Miltenyi Biotech, Germany) at a concentration of 300,000 cells / mL and strained with a  $20-\mu$ m mesh size Pre-Separation Filter (Miltenyi Biotech, Germany). Cell solution, up to a maximum of 10~mL, was injected into the input chamber of the cartridge and warmed to  $37^{\circ}$ C. Physiological temperature was maintained throughout all experiments.

Depending on the  $\mu$ Hammer design used, the compressed NPCs experienced either a moderate strain of  $42.2\% \pm 7.4\%$  or a high strain of  $69.2\% \pm 12.1\%$  for durations of  $10~\mu$ s or  $100~\mu$ s. Equation (1) provides an estimate of the strain magnitude using the final gap closure,  $H_{gap}$  (determined by pincer height) and the measured mean cell diameter, d.

$$\varepsilon = (d - H_{gap})/d \times 100\% \tag{1}$$

TABLE I

NPC EXPERIMENTAL CONDITIONS

Parameter	Control	Sham	Compressed			
Strain Magnitude ε (%)	0	0	42	42	69	69
Strain Duration (µs)	0	0	10	100	10	100

Equation (2) provides an estimate of the strain rate from the ratio of the  $\mu$ Hammer actuation velocity,  $\nu$ , and mean cell diameter. In all compression conditions, cells experienced similar applied strain rates of  $\dot{\epsilon} \sim 200 \times 10^3 \text{ s}^{-1} \pm 36 \times 10^3 \text{ s}^{-1}$ .

$$\dot{\varepsilon} = v / d \tag{2}$$

Two control populations were analyzed for each experiment. In the sham condition, cells were flowed through the  $\mu$ Hammer device without electromagnetic actuation of the  $\mu$ Hammer impact face and subsequent cell compression. In the control condition, cells were never injected into the  $\mu$ Hammer cartridge, but were instead cultured and analyzed alongside the sham and compressed conditions. Table I lists all experimental conditions compared in this report.

#### D. Plasma Membrane Permeability Assay

To investigate the immediate loss of membrane integrity due to mechanical injury, the membrane impermeable fluorescent marker Propidium Iodide (PI, Sigma-Aldrich, USA) (5% v/v) was added to each group upon retrieval from the output chamber. Flow cytometry was used to detect fluorescence due to PI intake by cells in each sampled population (populations ≥ 50,000 cells/sample), where higher PI fluorescence would indicate increased plasma membrane damage. To assess membrane damage immediately after cell impact, treatment groups were investigated within five minutes of removal from the output chamber. For each condition, three population replicates were analyzed per experiment, with the experiment repeated in triplicate.

#### E. Apoptosis Assay

To investigate early apoptosis, cells from all groups were seeded in 48-well plates and cultured for 1 hour, 4 hours, or 24 hours. At each assessment time point, cells were enzymatically lifted by a brief incubation in diluted 1:10 Accumax (eBioscience, USA); after 3 minutes, the reaction was quenched by addition of media. Cells were centrifuged at 300g and washed with Annexin V Buffer (Invitrogen, USA). Cells were stained with Annexin V-FITC (Miltenyi Biotech, Germany) (10% v/v) in Annexin V Buffer for 15 minutes at 21°C. The stained cells were diluted 1:5 with Annexin V Buffer and PI was added (5% v/v). Flow cytometry was used to detect fluorescence signals of both Annexin V-FITC and PI in each population. For each experiment,  $n \ge 2$  wells for each time point and group were analyzed, with the experiment repeated in triplicate.

## F. Proliferation Assay

To track the growth of cells after impact, all groups were seeded in 96-well plates at 6,600 viable (PI<sup>-</sup>) cells/well and cultured for 4 days. At least twice daily, the cell number was quantified to track proliferation. For each time point, cells from 3 wells per condition were enzymatically lifted (1:10 Accumax, digestion for 3 minutes at 37°C, followed by media quench). Cell density was measured using flow cytometry by quantifying the average cell number harvested from each well. Up to four experimental replicates were conducted.

Equation (3) was used to normalize the quantified cell populations. For each time point, i, the ratio of the mean cell number, N, for each treatment group, j, to the mean cell number of the corresponding experiment control,  $N_{j'}$ , was calculated as follows.

$$N/N_{\text{Control}} = N_{j,i}/N_{j',i} \tag{3}$$

Equations (4) and (5) were used to compare the proliferation rate of each condition. The doubling time,  $t_{\text{double}}$ , of each condition, j, was estimated by the exponential growth rate,  $r_j$ , determined using a linear regression of the natural log transformed exponential phase. The exponential phases typically initiate at  $t_1 \simeq 24$  hours and end at  $t_{\text{final}} \simeq 75$  hours after seeding this cell line.

$$t_{\text{double,j}} = \ln(2)/r_{\text{j}}$$
 (4)

$$\ln\left(N_{\mathbf{i},t}\right) = \ln\left(N_{\mathbf{i},\mathbf{t}_1}\right) + r_{\mathbf{i}}t\tag{5}$$

# G. Statistics

Statistical comparisons between compressed, sham, and the control groups were performed using One-way ANOVA and post-hoc Dunnett's test,  $\alpha=0.05$ . Differences within compressed groups were also statistically evaluated to decouple the effect of strain magnitude and strain duration, performed using Two-way ANOVA,  $\alpha=0.05$ . All statistics were performed using GraphPad Prism v 8.0.

# III. RESULTS

# A. Strain Magnitude Increases Membrane Permeability

The mechanical injury from  $\mu$ Hammer compression resulted in an immediate and significant increase in membrane permeability for NPCs (Fig. 2a). Each strained condition had increased population of the percentage of PI positive cells (% PI<sup>+</sup>) compared to the control group. To rule out effects of flow-induced shear stress, we compared the sham and control conditions and found no statistical difference. We then examined the effect of strain magnitude and durations (Fig. 2b) on membrane integrity. We found that the magnitude of applied strain had a significant effect on % PI<sup>+</sup> population, with increased damage at the higher strain magnitudes. By contrast, there was no significant difference between the % PI<sup>+</sup> cells for different strain durations at a fixed strain magnitude.

### B. Strain Duration Initiates Early Apoptosis

One of the first distinguishing events of apoptosis (programmed death), is the translocation of the membrane-bound phospholipid, phosphatidylserine (PS), from the inner to outer

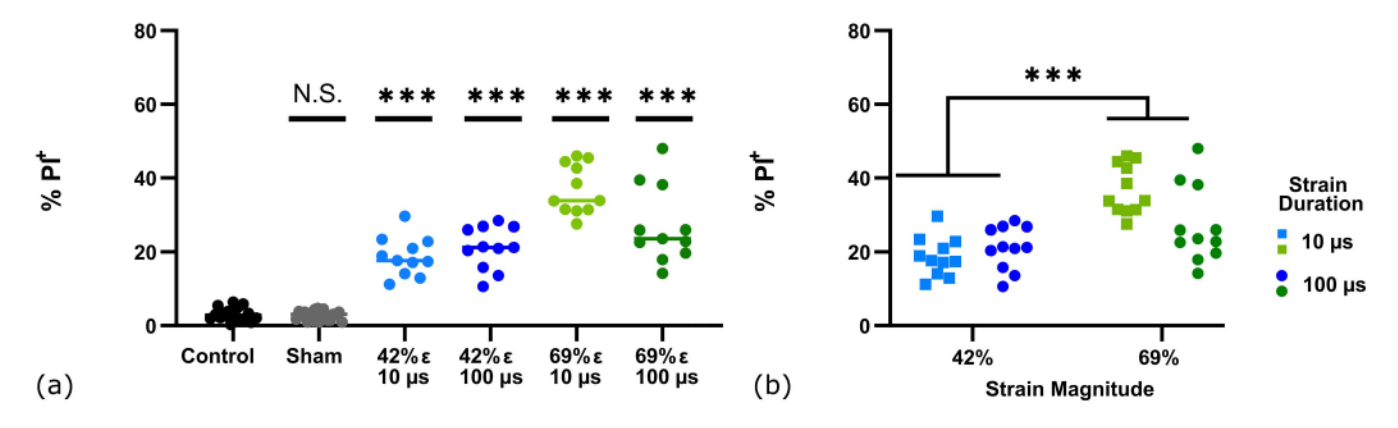


Fig. 2. (a) The percent of PI positive (PI<sup>+</sup>) stained cells, with statistical comparison of each group to the control. Each point represents a sampled population of at least  $5 \times 10^4$  cells. Colored line depicts mean across 3 experimental replicates for each group (b) Comparing within compressed groups and showing the sensitivity of response to strain magnitude, not duration. N.S. = no significant difference, \*\*\* = p < 0.01.

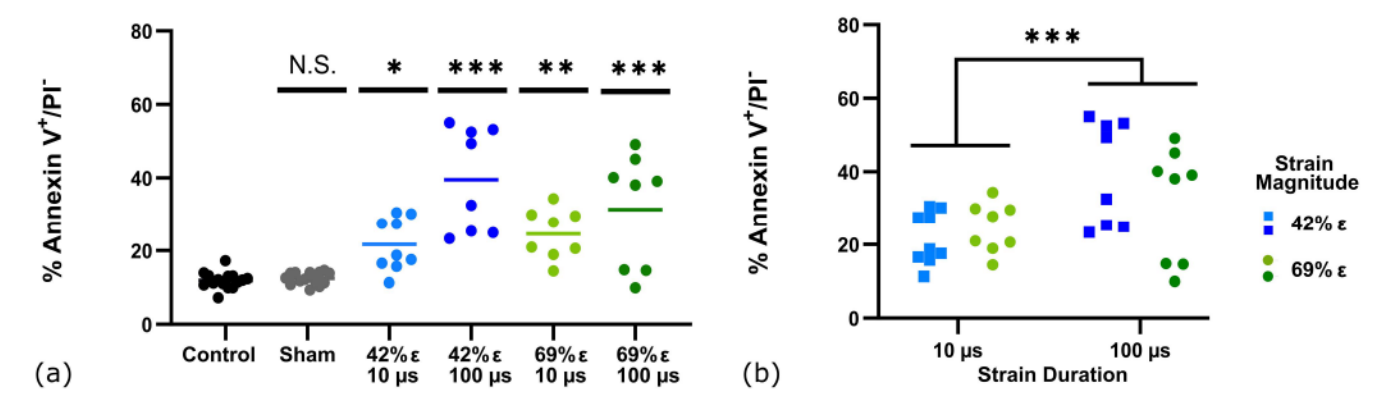


Fig. 3. (a) The percentage of cells detected as Annexin  $V^+/PI^-$  (early apoptotic) 24 hours after seeding, with statistical comparisons of each group to the control. Each point represents a sampled population from an individual well. The colored line depicts mean across three experimental replicates for each group. (b) Comparing within compressed groups at 24 hours to show the sensitivity of response to strain duration but not magnitude. N.S. = no significant difference, \* = p < 0.1, \*\* = p < 0.05, \*\*\* = p < 0.01.

leaflet of the plasma membrane. This exposed PS can be monitored by the binding of fluorescently conjugated Annexin V protein. Here, cells were identified as positive for Annexin V-FITC binding (Annexin  $V^+$ ), but with intact plasma membranes (PI $^-$ ), a state representative of early apoptosis.

Neither the 1-hour nor 4-hour time points showed a significant change in the % Annexin V<sup>+</sup>/PI<sup>-</sup> population compared to the control condition, although all compressed groups showed an increase in early-phase apoptosis after 4 hours of culture compared to 1 hour of culture. After 24 hours of culture, all compression conditions showed significantly increased early apoptosis relative to the control (Fig. 3a). Interestingly, strain duration had a significant effect on early apoptosis, while strain magnitude had no effect (Fig. 3b). There was no significant difference between the sham and the control populations, indicating that flow-induced shear stress alone did not induce apoptosis.

As cells continue to progress through additional stages of apoptosis, the plasma membrane eventually breaks down. The stage of late apoptosis was identified as a cell positive for both Annexin V and PI. There was no significant difference in late apoptosis (Annexin  $V^+/PI^+$ ) across all time points. There was also no significant difference in necrosis (Annexin  $V^-/PI^+$ ),

though this could be attributed to dead cells lost from the sample populations during the low-speed centrifugation step.

# C. Strain Duration Reduces Cell Number, With No Effect on Proliferation Rate

NPCs were cultured for four days, with cell growth quantified at least twice daily. Representative results from one of the four experimental replicates are shown in Fig. 4a, depicting the average cell number over 70 hours of culture. The sham condition most closely compares to the control at each time point. The compressed groups have fewer cells than the control and sham for all time points after seeding. Despite this, across all experiments there is no significant difference in doubling times between any compression group and the control (Fig. 4a, inset). The control group doubling times range from 15 hours to 25 hours, demonstrating the experimental variability which could obscure inter-group differences in proliferation rate.

To attempt to reduce the effects of experimental variability on cell growth, the cell number, N, for each treatment group is normalized to its respective experimental control,

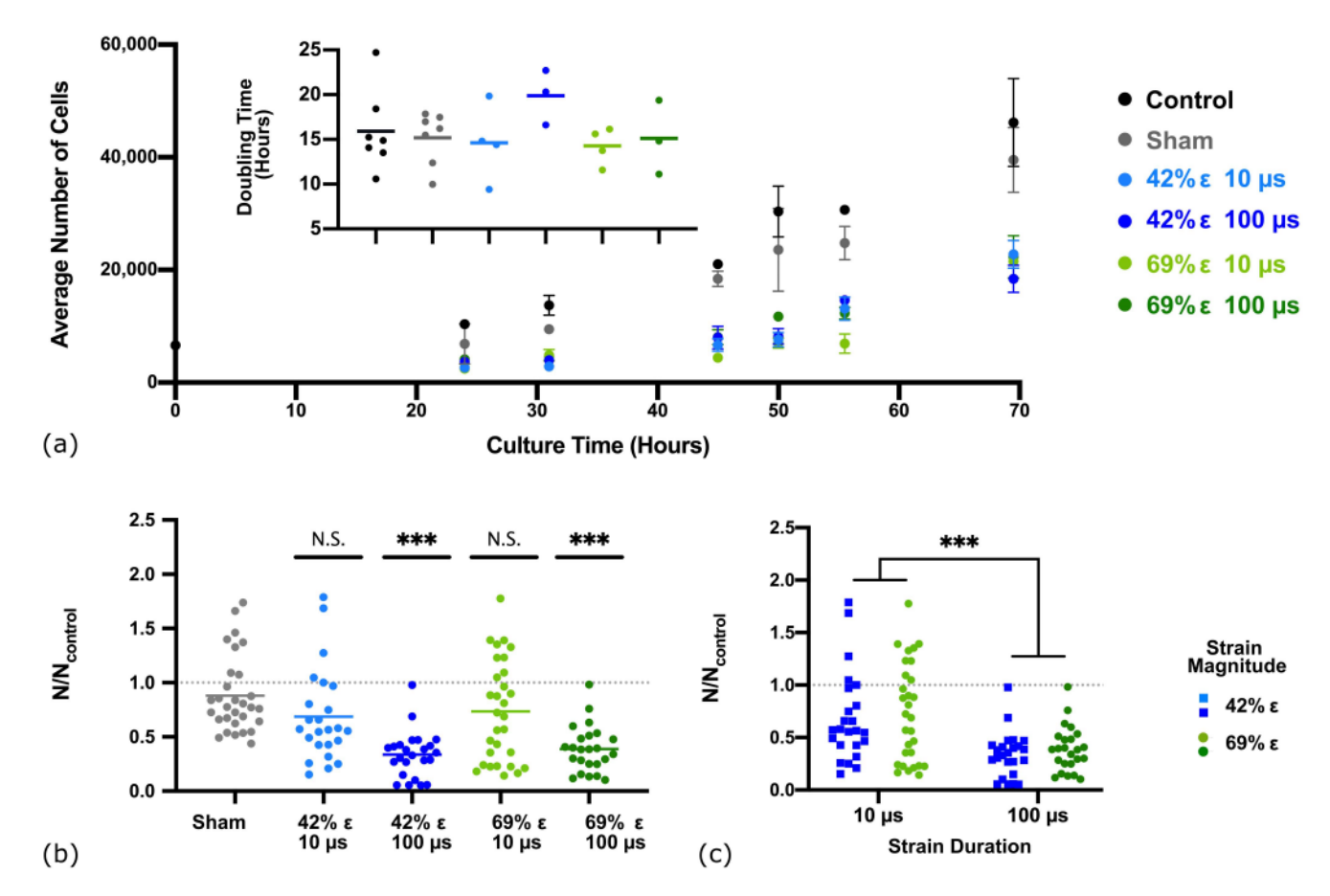


Fig. 4. Effect of compression on NPC proliferation. (a) Plot of representative data from 1 experimental replicate, showing mean number of cells over a 70-hour period, error bars reflect standard deviation across n=3 wells. Inset depicts the doubling times calculated from  $n \ge 3$  experiments, with no significant differences. (b) Ratio of mean cell number for each treatment condition to control, with each point representing ratio for single time point, colored line depicts mean of  $N \ge 24$  time points, across  $n \ge 3$  experimental replicates. Cells compressed for  $100\mu s$  have significantly lower normalized cell numbers compared to cells subjected to the sham condition. (c) Comparing within compressed groups, significantly lower normalized cell growth is correlated to strain duration. N.S. = no significant difference, \*\*\* = p < 0.01.

 $N_{control}$  (Figure 4b). In this plot, each time point is depicted as a point, the mean for each group a line. The treatment groups all have mean  $N/N_{control} < 1$ . Moreover, compressed groups had  $N/N_{control}$  ratios significantly lower than the sham for two conditions:  $\varepsilon = 42\%$ -100  $\mu$ s, and  $\varepsilon = 69\%$ -100  $\mu$ s. Thus, in comparing within compressed groups, we found increasing the strain duration significantly decreased  $N/N_{control}$  (Fig. 4c).

#### IV. DISCUSSION

The  $\mu$ Hammer was used to investigate the effects of mechanical strain injury when applied to individual human-derived NPCs. Using magnetic actuation and microfluidics, up to 36,000 cells were impacted each minute, enabling the analysis of large populations of injured cells. Applying consistent injury impact parameters allowed for statistically robust analysis of changes in NPC membrane permeability, early apoptosis, and proliferation.

Plasma membrane degradation is a typical precursor to necrosis (cell death), although prior studies have shown conflicting trends regarding effects of mechanical damage. Previous studies report sustained loss of cell viability after stretch injury [15], [16]. On the other hand, membrane repair

of neuronal cells has been shown to occur within 10 minutes of stretch injury [17] and impermeable dye uptake has been found to decrease over a 24-hour period after injury [18]. We find that cell membrane permeability significantly increased immediately after compression and higher applied strains corresponded to a larger number of injured cells, assessed by higher % PI<sup>+</sup>. Since membrane damage was measured within five minutes after compression, this observation suggests that primary cellular injury, rather than a biomolecular cascade related to secondary injury, was responsible for membrane damage. These results are consistent with previous *in vitro* cell stretch studies that showed strain magnitude governs cellular uptake of impermeable dyes [15]–[18].

At 24 hours after injury, compressed NPCs demonstrated a significant increase in early apoptosis compared to the control group cells. This increase in apoptotic markers was significantly correlated to strain duration. For  $\varepsilon=42\%$  increasing strain duration from 10  $\mu s$  to 100  $\mu s$  resulted in a 1.8-fold increase in mean early apoptosis. For  $\varepsilon=69\%$  there was a 1.3-fold increase with increased strain duration. To our knowledge, no prior cell compression study has reported scaled cellular response to a difference in injury duration on the order of microseconds.

The apoptotic pathway varies for different cell types and stimuli [19]; therefore three timepoints were chosen over 24 hours to increase the chance of capturing the induction of apoptosis. While previous stretch injury on neuronal cells showed significantly increased early apoptosis by four hours [20], cells compressed with the  $\mu$ Hammer were not significantly early apoptotic until the 24-hour timepoint. While late apoptosis was not detected within the first 24 hours after injury, future investigations will monitor apoptosis at later time points to determine whether injured cells recover from early apoptosis or progress into late apoptosis, and correlate these to strain magnitude or duration.

After compression, the cells were also cultured for four days and their number recorded over time. The normalized cell number across all time points was significantly reduced in cells strained for 100  $\mu$ s, whereas there was no significant change in cells strained for 10  $\mu$ s. We suspect that the reduced cell number is due to cell necrosis that occurred after seeding. These necrotic cell populations were undetected in the early apoptosis assay, likely due to removal of dead cells from the measured population during the additional processing step of the low-speed centrifugal wash, not included in the proliferation assay. While there was a correlation between strain duration and cell number during proliferation, the doubling times of compressed cells were not significantly different when compared to the control. The unaffected proliferation rate despite fewer cells in the population suggests that the mitotic capability of the non-necrotic cells was maintained after injury. Future experiments will directly test these hypotheses.

# V. Conclusion

The  $\mu$ Hammer MEMS device was used to investigate the effects of mechanical strain on human NPCs by applying strains of magnitude  $\varepsilon = 42\%$  or  $\varepsilon = 69\%$  for static periods of 10  $\mu$ s or 100  $\mu$ s. The high throughput, single-cell nature of the  $\mu$ Hammer MEMS device enabled measurement of the robust population statistics necessary for thorough investigation of cellular response to compressive injury. We report the influences of strain magnitude and duration across several biological injury assays. Strain magnitude was significantly correlated to increased membrane permeability within five minutes of cell compression, while strain duration was significantly correlated to longer timescale effects: early apoptosis at 24 hours after compression and cell number over four days of culture. Future work will continue to explore the transient mechanisms of cellular injury to improve our understanding of cellular damage and recovery.

#### ACKNOWLEDGMENT

The authors thank Robert Stegman from the Department of Molecular, Cellular, and Developmental Biology, UCSB, for his technical help in measuring NPC cell size.

# REFERENCES

 M. C. Dewan *et al.*, "Estimating the global incidence of traumatic brain injury," *J. Neurosurg.*, vol. 130, no. 4, pp. 1080–1097, Apr. 2019, doi: 10.3171/2017.10.JNS17352.

- [2] M. Galgano, G. Toshkezi, X. Qiu, T. Russell, L. Chin, and L.-R. Zhao, "Traumatic brain injury: Current treatment strategies and future endeavors," *Cell Transplantation*, vol. 26, no. 7, pp. 1118–1130, Jul. 2017, doi: 10.1177/0963689717714102.
- [3] J. Ramos-Cejudo et al., "Traumatic brain injury and Alzheimer's disease: The cerebrovascular link," EBioMedicine, vol. 28, pp. 21–30, Feb. 2018, doi: 10.1016/j.ebiom.2018.01.021.
- [4] M. C. Morganti-Kossmann, B. D. Semple, S. C. Hellewell, N. Bye, and J. M. Ziebell, "The complexity of neuroinflammation consequent to traumatic brain injury: From research evidence to potential treatments," *Acta Neuropathologica*, vol. 137, no. 5, pp. 731–755, May 2019, doi: 10. 1007/s00401-018-1944-6.
- [5] C. Xie et al., "The effect of simvastatin treatment on proliferation and differentiation of neural stem cells after traumatic brain injury," Brain Res., vol. 1602, pp. 1–8, Mar. 2015, doi: 10.1016/j.brainres. 2014.03.021.
- [6] T.-S. Yu, G. Zhang, D. J. Liebl, and S. G. Kernie, "Traumatic brain injury-induced hippocampal neurogenesis requires activation of early nestin-expressing progenitors," *J. Neurosci.*, vol. 28, no. 48, pp. 12901–12912, Nov. 2008, doi: 10.1523/JNEUROSCI.4629-08. 2008.
- [7] S. Y. Ng and A. Y. W. Lee, "Traumatic brain injuries: Pathophysiology and potential therapeutic targets," *Frontiers Cellular Neurosci.*, vol. 13, Nov. 2019, doi: 10.3389/fncel.2019.00528.
- [8] D. K. Cullen, C. M. Simon, and M. C. LaPlaca, "Strain rate-dependent induction of reactive astrogliosis and cell death in three-dimensional neuronal–astrocytic co-cultures," *Brain Res.*, vol. 1158, pp. 103–115, Jul. 2007, doi: 10.1016/j.brainres.2007.04.070.
- [9] A. B. Shrirao et al., "Microfluidic platforms for the study of neuronal injury in vitro," Biotechnol. Bioeng., vol. 115, no. 4, pp. 815–830, Apr. 2018, doi: 10.1002/bit.26519.
- [10] B. Morrison, B. S. Elkin, J.-P. Dollé, and M. L. Yarmush, "In vitro models of traumatic brain injury," Annu. Rev. Biomed. Eng., vol. 13, no. 1, pp. 91–126, Aug. 2011, doi: 10.1146/annurev-bioeng-071910-124706.
- [11] M. Skotak, F. Wang, and N. Chandra, "An in vitro injury model for SH-SY5Y neuroblastoma cells: Effect of strain and strain rate," J. Neurosci. Methods, vol. 205, no. 1, pp. 159–168, Mar. 2012, doi: 10. 1016/j.jneumeth.2012.01.001.
- [12] J.-P. Dollé, B. Morrison, R. S. Schloss, and M. L. Yarmush, "Brain-on-a-chip microsystem for investigating traumatic brain injury: Axon diameter and mitochondrial membrane changes play a significant role in axonal response to strain injuries," *Technology*, vol. 2, no. 2, pp. 106–117, Jun. 2014, doi: 10.1142/s2339547814500095.
- [13] L. H. C. Patterson et al., "The μhammer: Investigating cellular response to impact with a high throughput microfluidic MEMS device," in Proc. Solid-State Sens., Actuators Microsyst. Workshop Hilton Head, 2018, pp. 167–170, 2018, doi: 10.31438/trf.hh2018.47.
- [14] L. H. C. Patterson et al., "Investigating cellular response to impact with a microfluidic MEMS device," J. Microelectromech. Syst., vol. 29, no. 1, pp. 14–24, Feb. 2020, doi: 10.1109/JMEMS.2019. 2948895.
- [15] E. Bar-Kochba, M. T. Scimone, J. B. Estrada, and C. Franck, "Strain and rate-dependent neuronal injury in a 3D in vitro compression model of traumatic brain injury," Sci. Rep., vol. 6, no. 1, pp. 1–11, Aug. 2016, doi: 10.1038/srep30550.
- [16] D. K. Cullen and M. C. LaPlaca, "Neuronal response to high rate shear deformation depends on heterogeneity of the local strain field," *J. Neu-rotrauma*, vol. 23, no. 9, pp. 1304–1319, Sep. 2006, doi: 10.1089/neu. 2006.23.1304.
- [17] D. M. Geddes, R. S. Cargill, and M. C. LaPlaca, "Mechanical stretch to neurons results in a strain rate and magnitude-dependent increase in plasma membrane permeability," *J. Neurotrauma*, vol. 20, no. 10, pp. 1039–1049, Oct. 2003, doi: 10.1089/089771503770195885.
- [18] J. S. McKinney, K. A. Willoughby, S. Liang, and E. F. Ellis, "Stretch-induced injury of cultured neuronal, glial, and endothelial cells: Effect of polyethylene glycol-conjugated superoxide dismutase," *Stroke*, vol. 27, no. 5, pp. 934–940, May 1996, doi: 10.1161/01.STR. 27.5.934.
- [19] J. Wong, N. W. Hoe, F. Zhiwei, and I. Ng, "Apoptosis and traumatic brain injury," *Neurocrit. Care*, vol. 3, no. 5, pp. 177–182, 2005, doi: 10. 1385/NCC:3:2:177.
- [20] Y. Jing et al., "Neuroprotective effects of serpina3k in traumatic brain injury," Frontiers Neurol., vol. 10, pp. 1–11, Nov. 2019, doi: 10.3389/ fneur.2019.01215.



Jennifer L. Walker (Graduate Student Member, IEEE) received the B.S. degree in bioengineering from Rice University in 2016. She is currently pursuing the Ph.D. degree with the Foster Mechanics of Microscale Systems Laboratory, University of California at Santa Barbara (UC Santa Barbara), Santa Barbara, CA, USA.

As an undergraduate, she was a member of the Mikos Research Group, where she focused on tissue engineering and biomaterials for drug delivery. She also conducted MEMS research at the Laboratory

of Kimberly Foster, UC Santa Barbara, and Owl Biomedical, Santa Barbara. Her research focuses on the development and application of a high-throughput MEMS device for controllably subjecting individual cells to large deformation in order to link mechanical injury to the progression of neural disease.



John S. Foster received the B.A. degree in physics from the University of California at San Diego in 1980 and the Ph.D. degree in applied physics from Stanford University in 1984.

He was the Chief Operating Officer of Applied Magnetics Corporation and the Vice President of Worldwide Operations. He was the Managing Director of Applied Magnetics Malaysia. At IBM, he served as a Product Manager and the Research and Development Manager. He was on the faculty at Stanford University in applied physics. He was

the Chief Executive Officer, the Chairman, and the Co-Founder of Innovative Micro Technology. He is currently the President and Co-Founder of Owl Biomedical (now a subsidiary of Miltenyi Biotec). He holds 60 patents.



Luke H. C. Patterson (Graduate Student Member, IEEE) received the B.S. degree in engineering physics from Westmont College in 2014. He is currently pursuing the Ph.D. degree in mechanical engineering with the Foster Mechanics of Microscale Systems Laboratory, University of California at Santa Barbara (UC Santa Barbara).

He is currently a Department Merit Fellow and a Teaching Assistant with the Mechanical Engineering Department, UC Santa Barbara. His research focuses on developing MEMS technology to better under-

stand and ultimately treat traumatic brain injury (TBI).



Megan T. Valentine received the B.S degree from Lehigh University, the M.S. degree from the University of Pennsylvania, and the Ph.D. degree from Harvard University, all in physics.

She completed a Post-Doctoral Fellowship in biological sciences at Stanford University, with the support of a Damon Runyon Cancer Research Fellowship and a Burroughs Wellcome Career Award. She is currently a Professor of mechanical engineering with the University of California at Santa Barbara (UC Santa Barbara) and an Associate

Director of the California NanoSystems Institute, where she develops new tools for analysis of molecular and cellular mechanics and applies biological design principles to develop high-performance materials. Her major awards include the NSF CAREER Award and the Fulbright Scholar Award to ESPCI-ParisTech, France, to support her work on neuron mechanics and adhesion, respectively.

Dr. Valentine is a fellow of the American Physical Society.



Evelyn Rodriguez-Mesa received the B.S. degree in cellular biology from the Central University of Venezuela in 2005.

She has been a Senior Applications Scientist with Owl Biomedical since 2011. She previously worked at the Fred Hutchinson Cancer Research Center as a Research Technician in 2008. Her research has been focused on developing cell sorting strategies using the MACSQuant Tyto to assist new and current cell therapies in the treatment of cancer and other diseases. She published the textbook *Molecular Biology* 

of the Cell (May 1, 2015) and holds a technology patent, FHCRC Ref.10-012: Antibody to recognize the human WASH family of WAS protein.



Adele M. Doyle received the B.S. degree in biomedical engineering from Washington University at St. Louis and the Ph.D. degree from the Joint Biomedical Engineering Program, Georgia Institute of Technology and Emory University.

She completed a Post-Doctoral Fellowship in systems biology at Harvard University. She is currently an Assistant Professor of mechanical engineering at the University of California at Santa Barbara (UC Santa Barbara) and a Faculty Member with the Center for Bioengineering and Neuroscience

Research Institute. Her group studies how stem cells and their derivatives respond to applied mechanical forces via molecular and behavioral changes, in particular related to the nervous system. Her research has been funded by the NSF, NIH, and the Regent's Junior Faculty Fellowship.



Kevin Shields received the B.S. degree in mechanical engineering from the University of California at Santa Barbara (UC Santa Barbara) in 2011.

In 2011, he began his professional career at Owl Biomedical as a Mechanical Engineer. He is currently a Senior Mechanical Systems Engineer with Owl Biomedical. His focus is on MEMS design and systems engineering for the MACSQuant Tyto cell sorting system. He is an inventor of five filed and two pending patents.



Kimberly L. Foster (Member, IEEE) received the B.S. degree in mechanical engineering from Michigan Technological University in 1994 and the Ph.D. degree in theoretical and applied mechanics from Cornell University in 1999.

In 1999, she joined the University of California at Santa Barbara (UC Santa Barbara), where she became a Full Professor in 2008. Among numerous positions, she served as the Department Chair from 2008 to 2013, co-chaired UCSB's BRAIN Initiative, and was the Associate Director of the Center for

Bioengineering, UCSB, until her departure in 2018. She is currently the Dean of the School of Science and Engineering, Tulane University. Her research focuses on the mechanics and nonlinear dynamics in microsystem and nanosystem, as well as on biomedical technology development. She has published over 175 refereed publications and received numerous awards, including the NSF CAREER Award and the UCSB Academic Senate Distinguished Teaching and Graduate Mentorship Awards.

Dr. Foster is a fellow of the ASME and the previous Chair of the MEMS Division. She was the Technical Program Chair and the General Chair of the Workshop for Solid-State Sensors and Actuators (Hilton Head) in 2008 and 2010, respectively.